

Supporting Information

Ultralong Needle-like N-doped Co(OH)F on Carbon Fiber Paper with Abundant Oxygen Vacancies as an Efficient Oxygen Evolution Reaction Catalyst

Jiaqi Lv, Xiaoxuan Yang, Hong-Ying Zang*, Yong-Hui Wang and Yang-Guang Li*

Key Lab of Polyoxometalate, Science of Ministry of Education, Key Laboratory of Nanobiosensing and Nanobioanalysis at Universities of Jilin Province, Institute of Functional Material Chemistry, Faculty of Chemistry, Northeast Normal University, Changchun, 130024, Jilin, P. R. China.

*Email: zanghy100@nenu.edu.cn; liyg658@nenu.edu.cn.

Table of Contents

Figure S1 SEM images of N:Co(OH)F-CFP in different sizes.

Figure S2 SEM images of material without NaF in different sizes.

Figure S3 LSV of N:Co(OH)F-CFP and N:Co(OH)F.

Figure S4 SEM images of IrO₂-CFP.

Figure S5 SEM-Mapping of N:Co(OH)F-CFP.

Figure S6 SEM of N:Co(OH)F-CFP after 10h IT stability test.

Figure S7 N₂ adsorption and desorption isotherm curve of the needle-like N:Co(OH)F-CFP.

Figure S8 (a) on the left side partial is N:Co(OH)F-CFP, the right is bare CFP.

(b) physical map of the test process. It's a schematic of a three-electrode device that actually reacts in 1M KOH.

Figure S9 Contact angle test chart for (a) bare CFP (b) N:Co(OH)F-CFP (c) N:Co(OH)F.

Figure S10 Co 2p and O1s XPS spectrum of N:Co(OH)_x-CFP(a,b), Co(OH)F-CFP(c,d) and Co(OH)_x-CFP(e,f).

Figure S11 Room-temperature photoluminescence spectra of N:Co(OH)F-CFP, N:Co(OH)_x-CFP, Co(OH)F-CFP and Co(OH)_x-CFP.

Figure S12 EDX of the array of N:Co(OH)F-CFP.

Figure S13 N:Co(OH)F-CFP of different amounts of NaF (a,b) and urea (c,d).

Figure S14. LSV of different urea and NaF ratios.

Figure S15 SEM of different time of N:Co(OH)F-CFP (a) 4h (b) 6h (c) 8h (d) 10h.

Figure S16. different reaction time of N:Co(OH)F-CFP.

Figure S17 LSV comparison of OER activity before and after IT testing.

Figure S18 (a) Electrochemical cyclic voltammetry of N:Co(OH)F-CFP at different sweep rates (voltage range: 0.12-0.32 V vs. RHE) (b) Double-layer capacitance curve of N:Co(OH)F-CFP and IrO₂-CFP.

Table S1 XPS full spectrum analysis of N:Co(OH)_x-CFP, Co(OH)F-CFP and Co(OH)_x-CFP.

Table S2 Comparison of selected Co-containing OER electrocatalysts for different substrates in alkaline media.

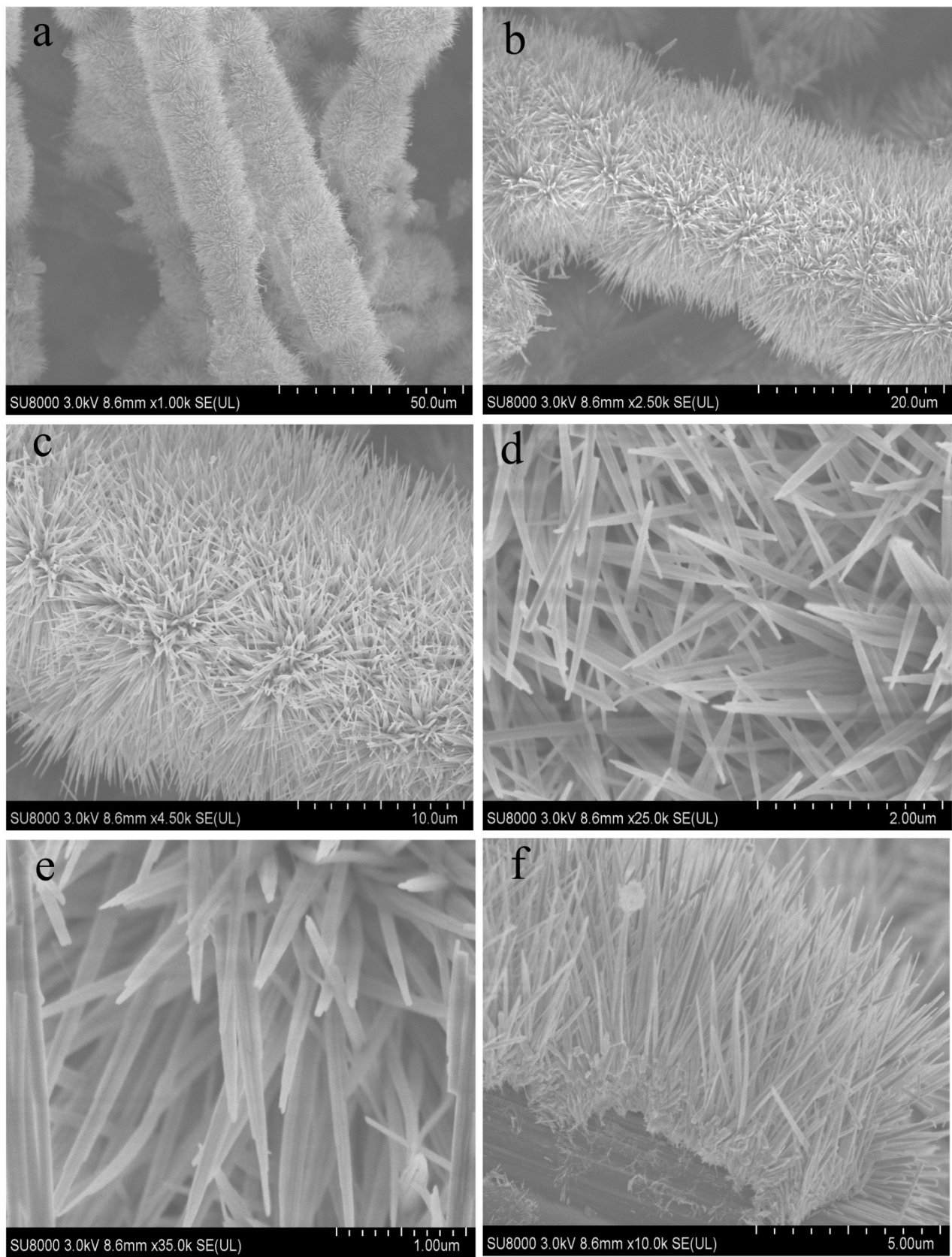


Figure S1. SEM images of N:Co(OH)F-CFP in different sizes.

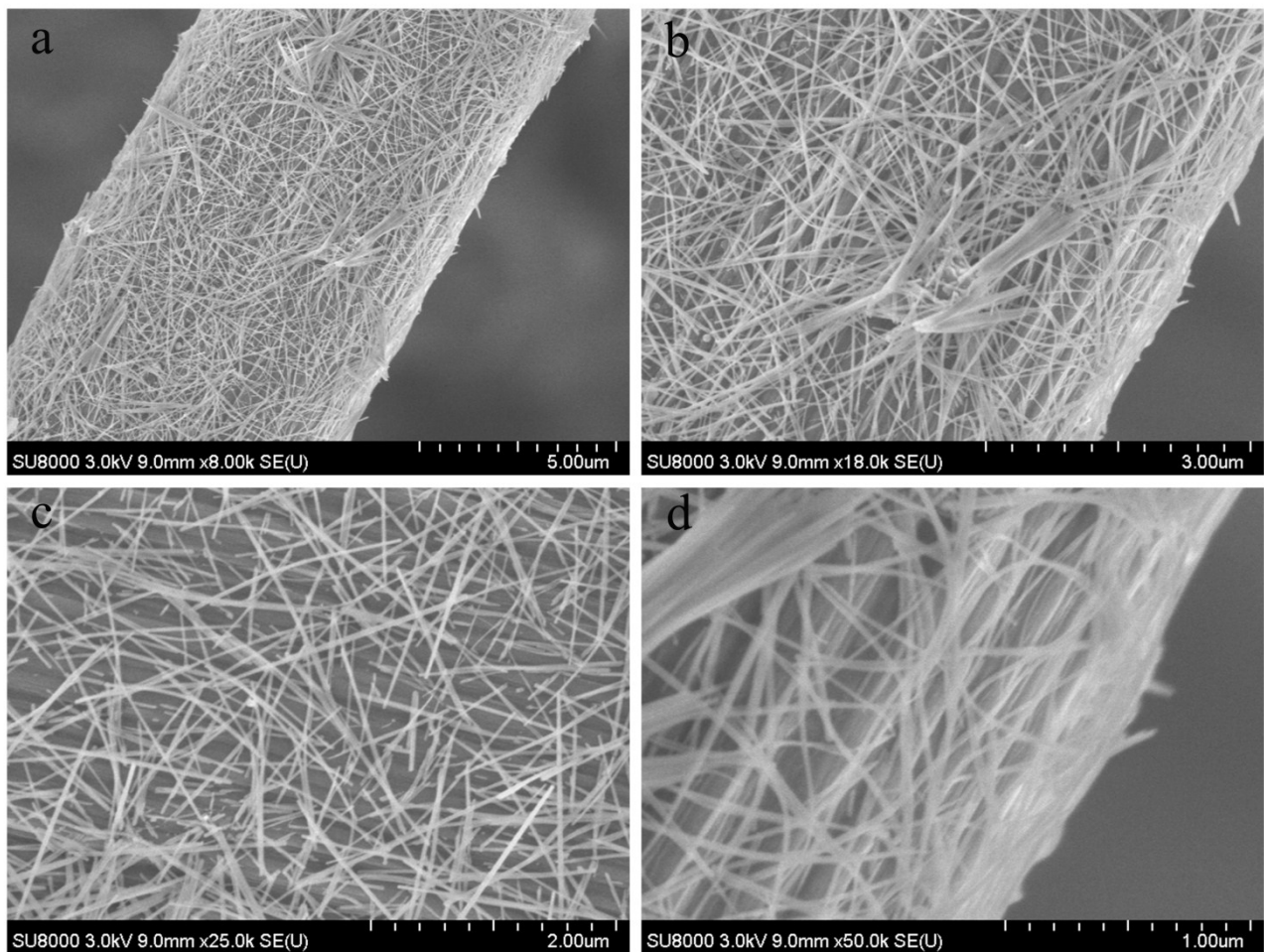


Figure S2. SEM images of material without NaF in different sizes.

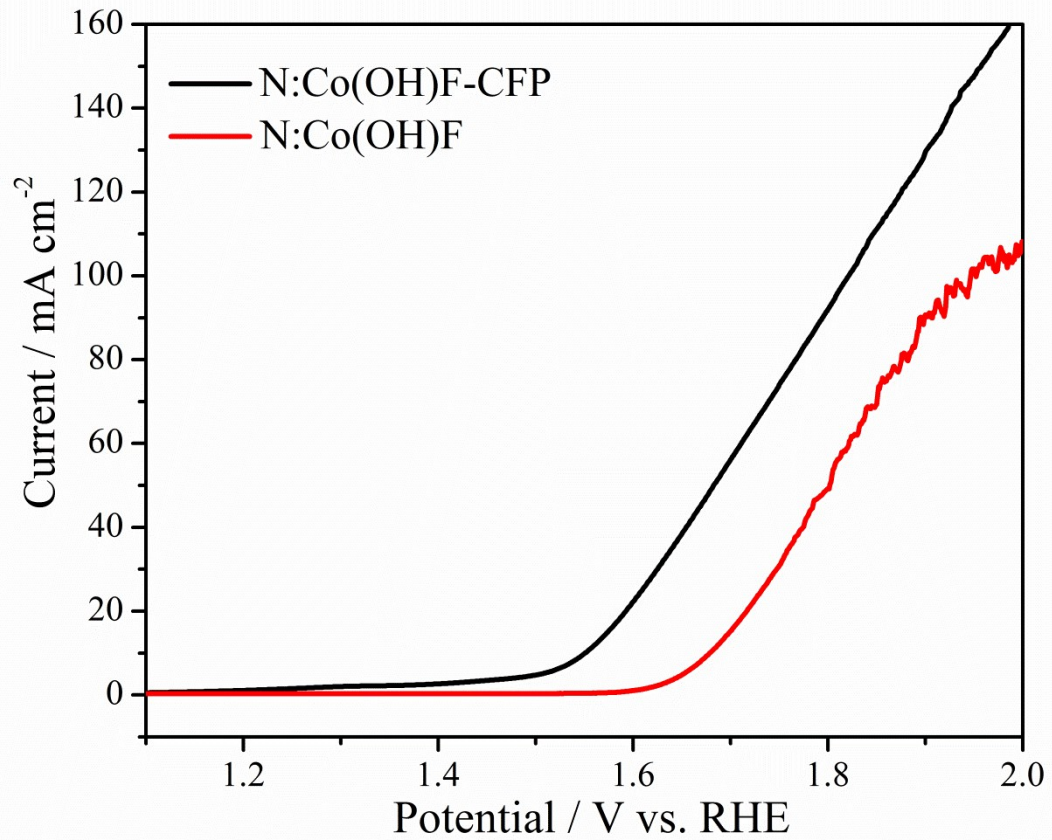


Figure S3. LSV of N:Co(OH)F-CFP and N:Co(OH)F.

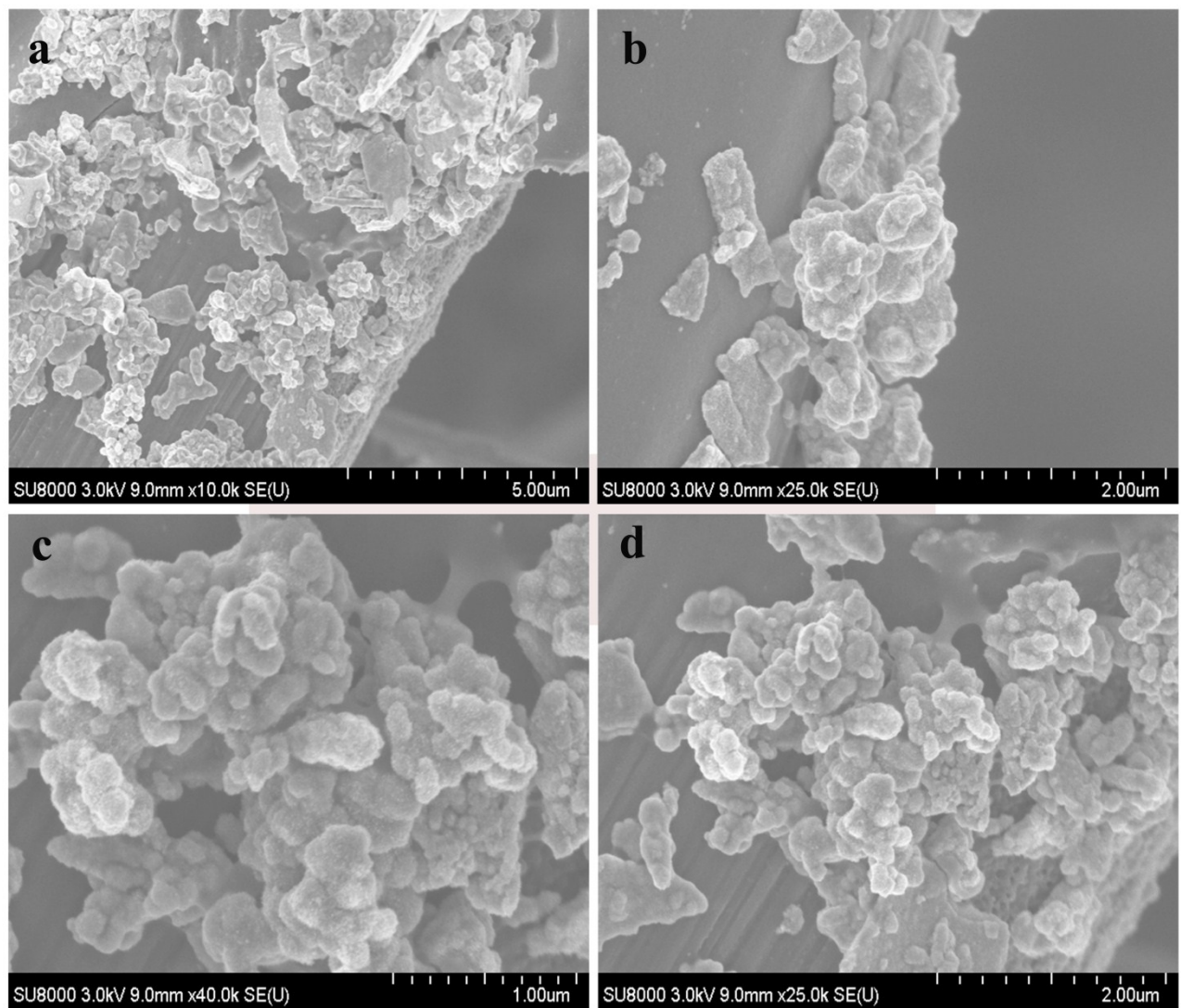


Figure S4. SEM images of IrO₂-CFP.

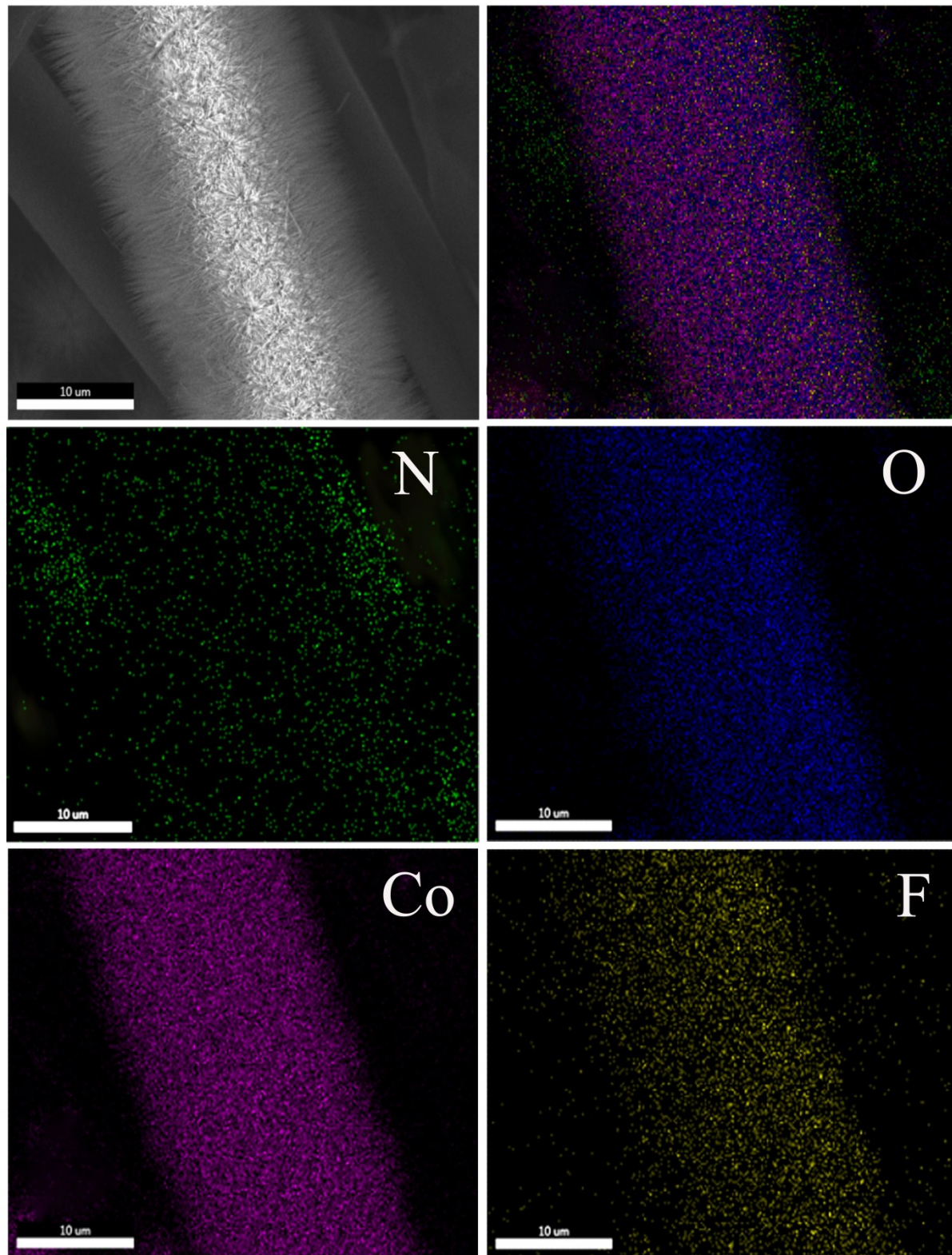


Figure S5. SEM-Mapping of the N:Co(OH)F-CFP.

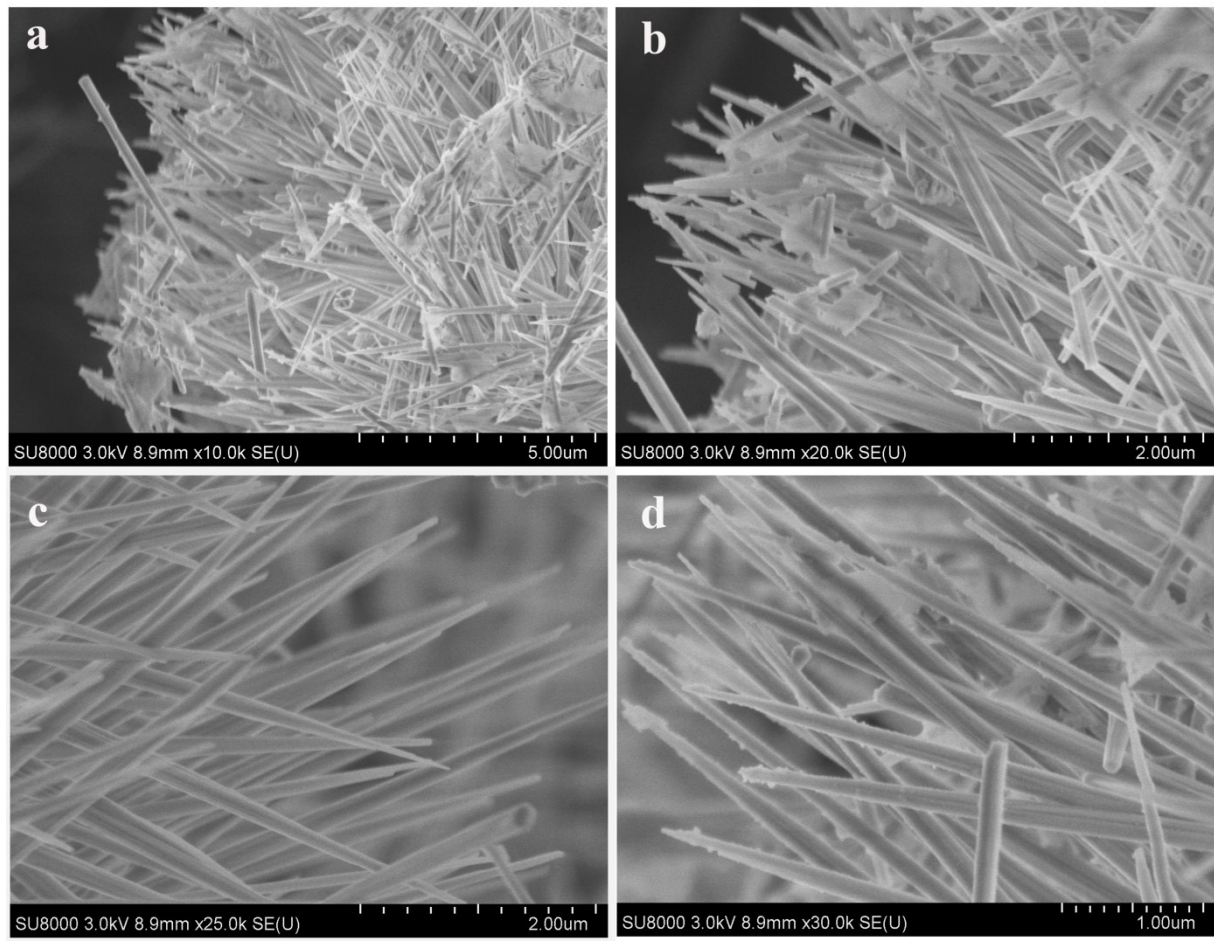


Figure S6. SEM of N:Co(OH)F-CFP after 10h IT stability test.

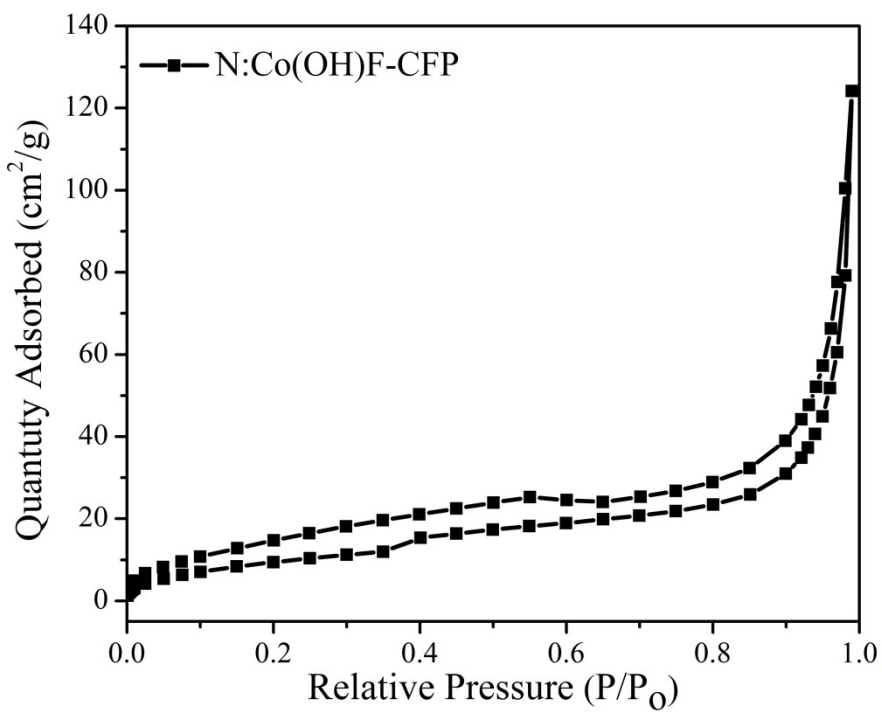


Figure S7. N_2 adsorption and desorption isotherm curve of the needle-like N:Co(OH)F-CFP.

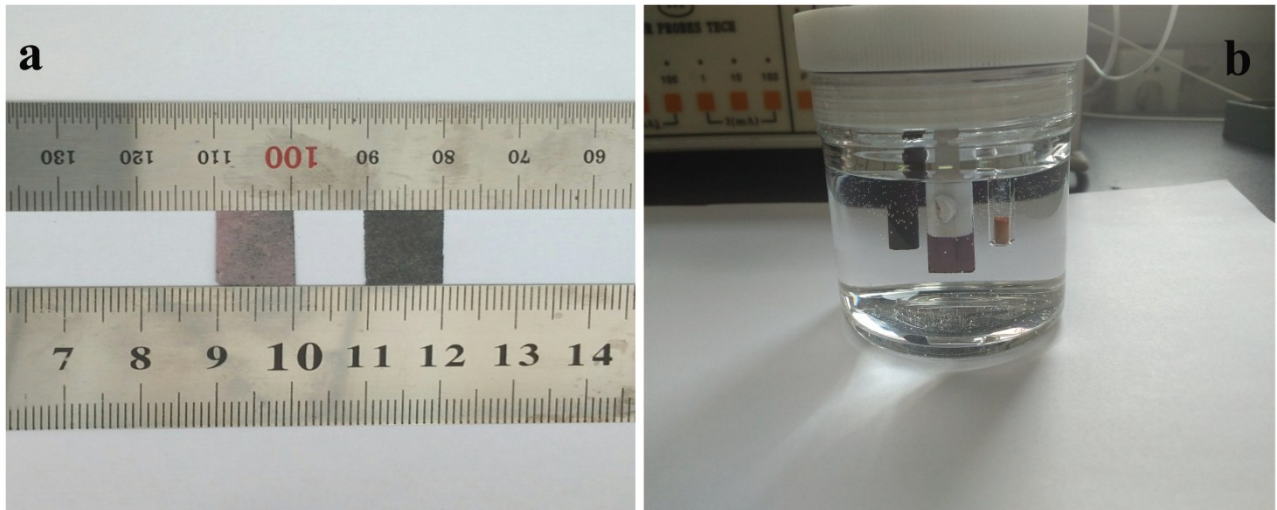


Figure S8. (a) on the left side partial is N:Co(OH)F-CFP, the right is bare CFP.
 (b) physical map of the test process. It's a schematic of a three-electrode device that actually reacts in 1M KOH.

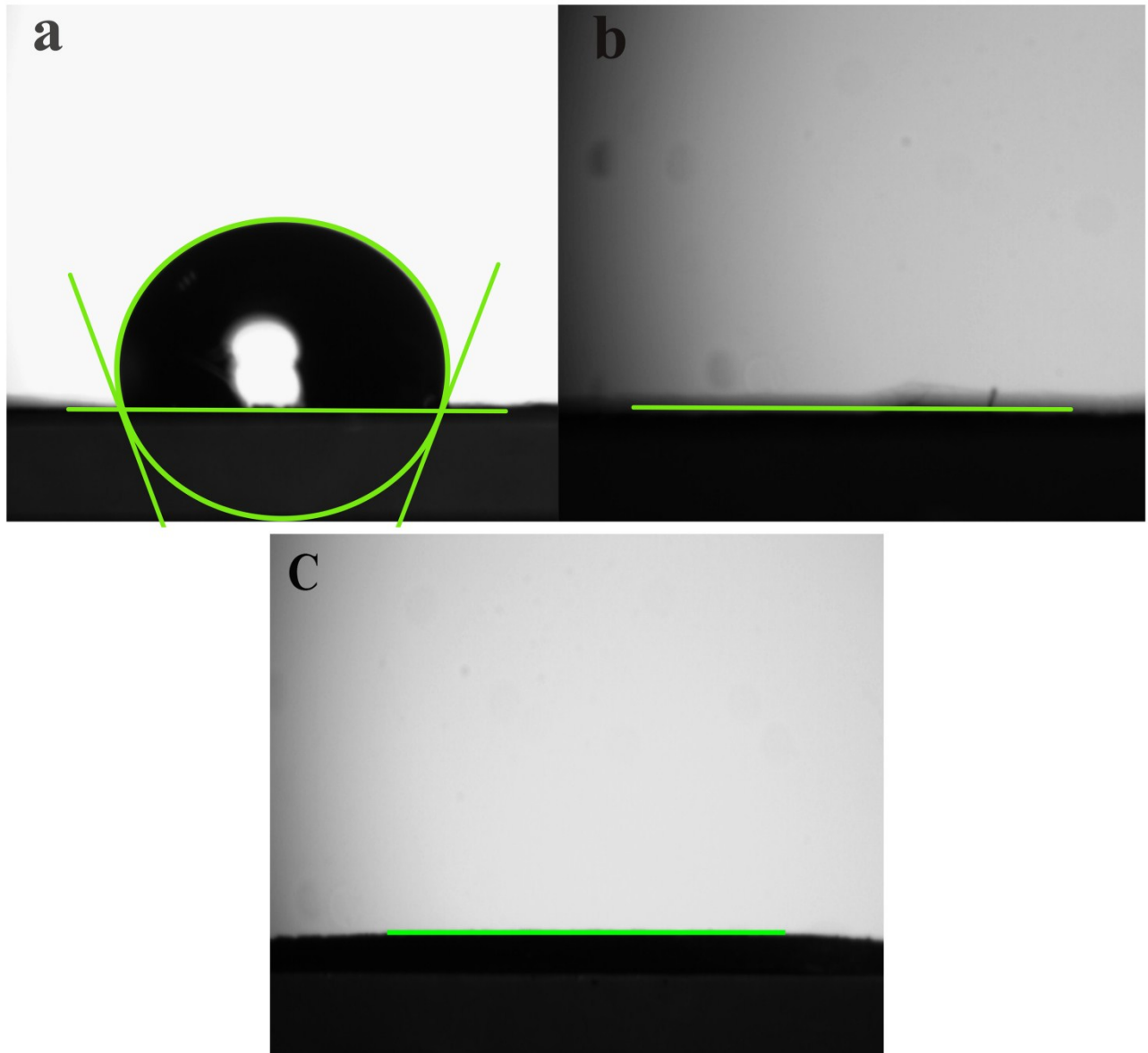


Figure S9. Contact angle test chart for (a) bare CFP (b) N:Co(OH)F-CFP (c) N:Co(OH)F.

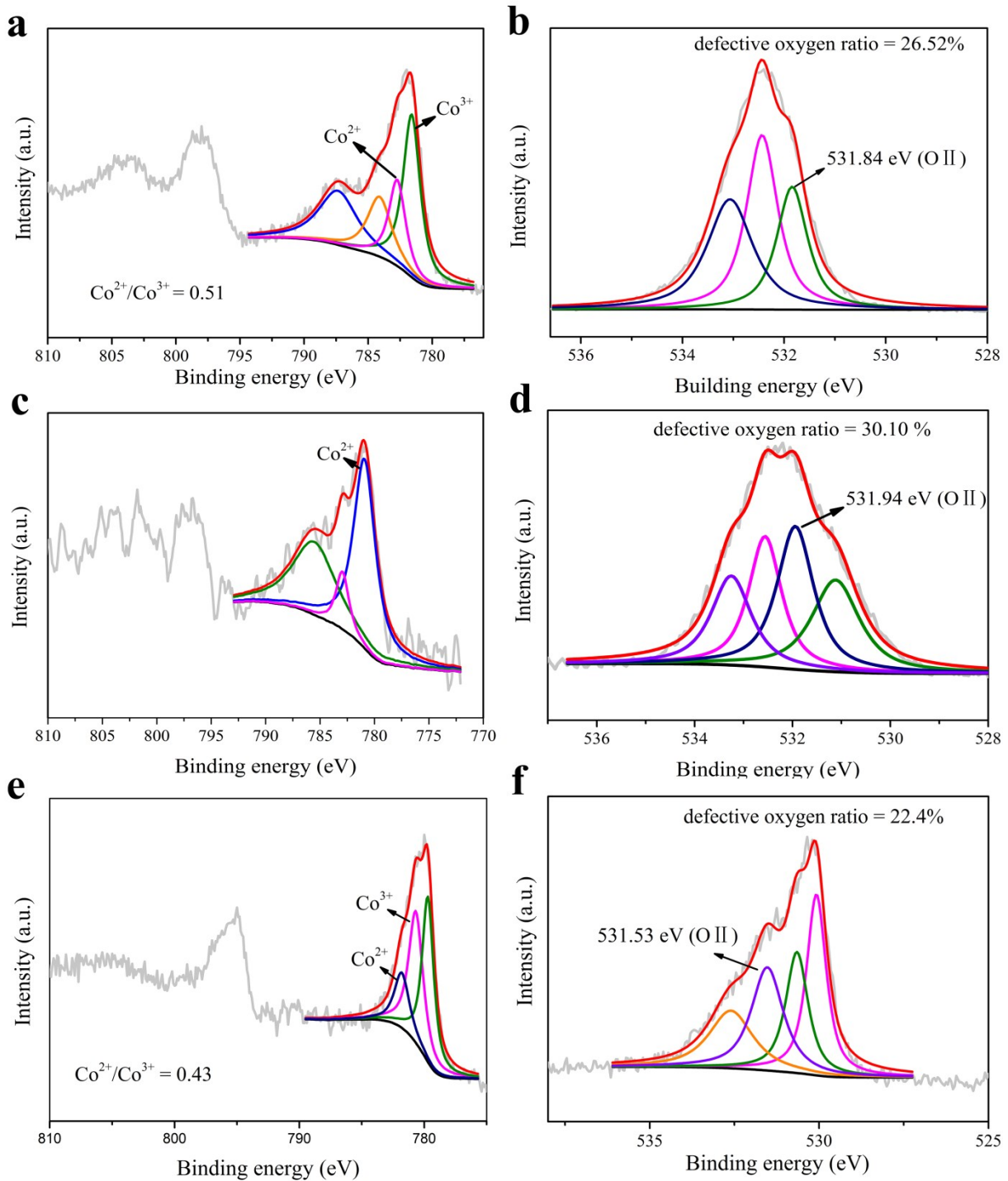


Figure S10. Co 2p and O1s XPS spectrum of N:Co(OH)_x-CFP(a,b), Co(OH)F-CFP(c,d) and Co(OH)_x-CFP(e,f).

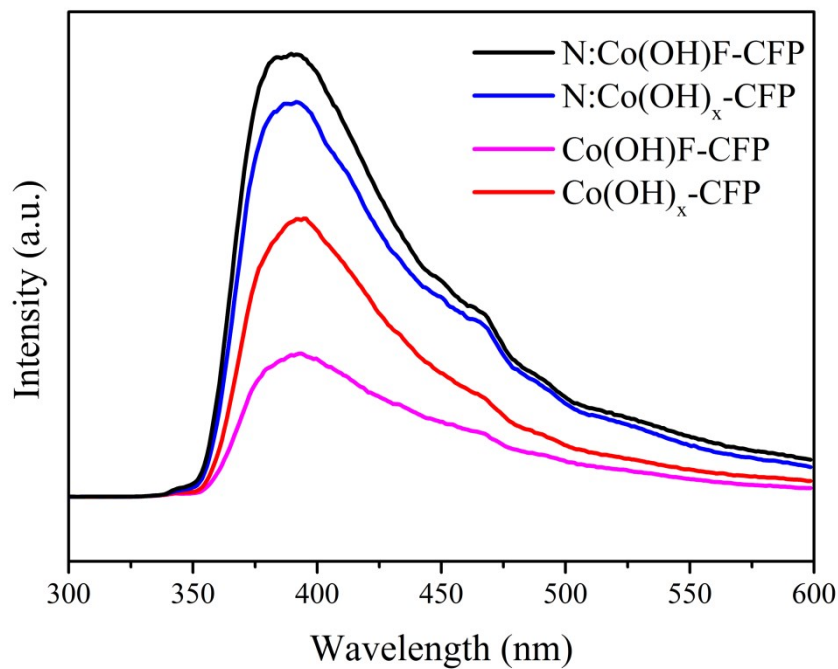
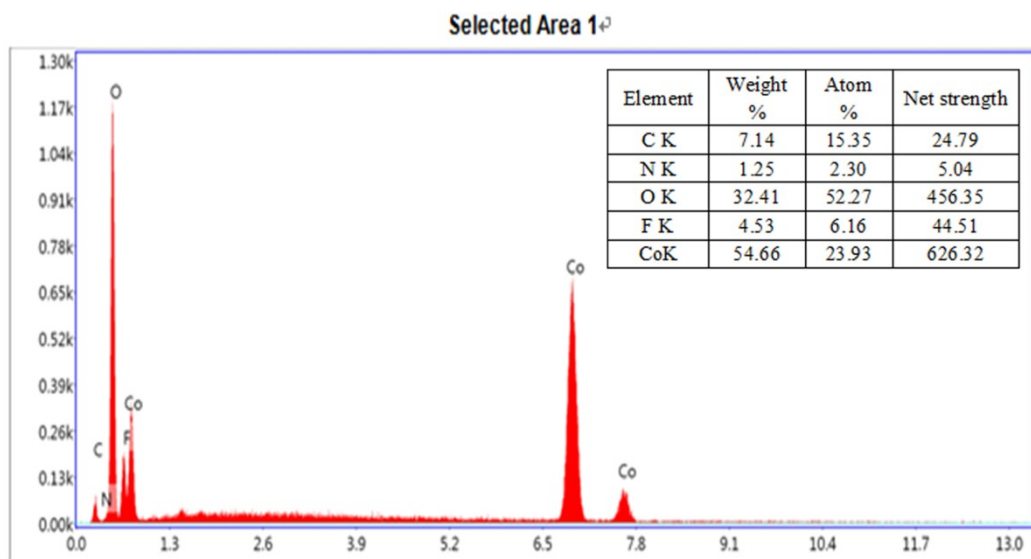


Figure S11. Room-temperature photoluminescence spectra of N:Co(OH)F-CFP, N:Co(OH)_x-CFP, Co(OH)F-CFP and Co(OH)_x-CFP.



Live time (s): 30.0 0 Cnts 0.000keV Detector: Apollo X-SDD Det

Figure S12. EDX spectroscopy of the array of N:Co(OH)F-CFP.

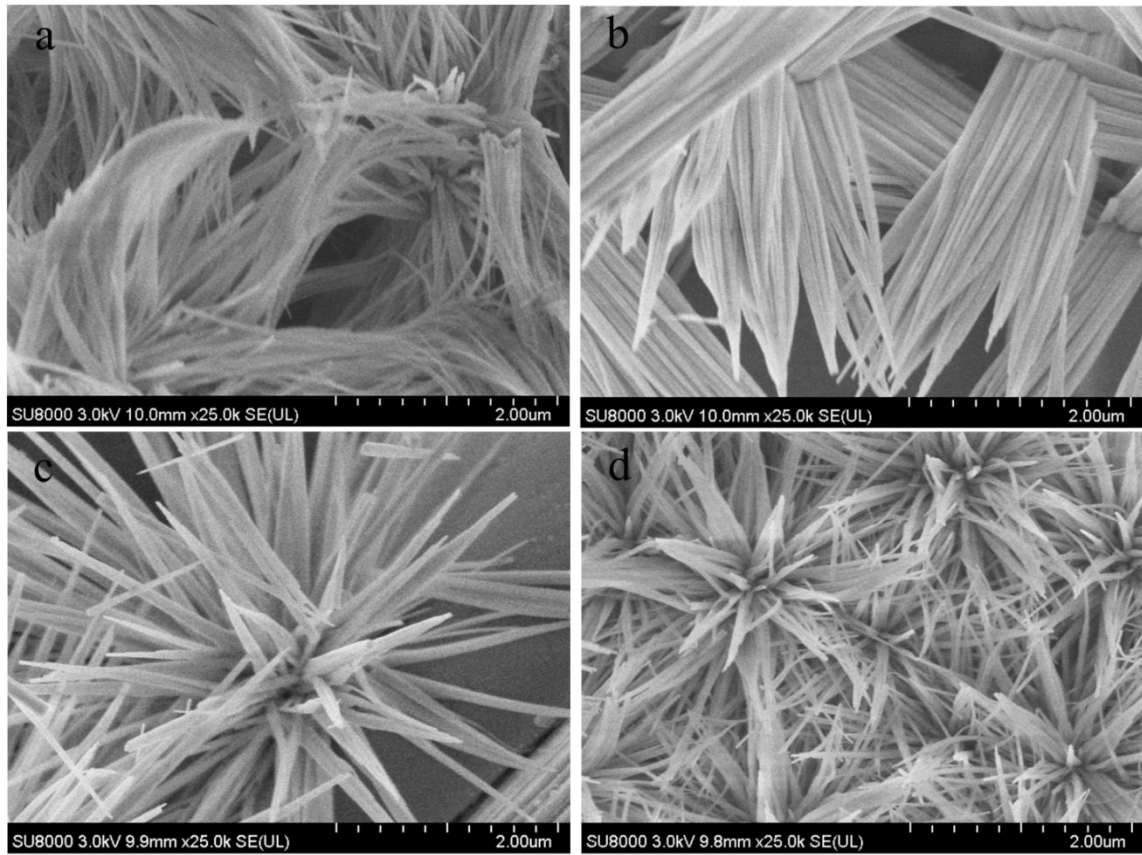


Figure S13. N:Co(OH)F-CFP of different amounts of NaF (a,b) and urea (c,d).

Figure S13 shows the effect of guiding reagents dose on the morphology of the material N:Co(OH)F. When the amount of halogen ion F⁻ was reduced to half of the original, N:Co(OH)F formed without acicular structure and was very soft (Figure S13a). Increasing the amount to double of the original, on the other hand, it will be a wider and fuller bar (Figure S13b). Urea is the major supplier of N in N:Co(OH)F, it did not form a uniform array on the CFP surface when reducing the dosage (Figure S13c). As the content of urea increased to double, we found it self-assembled flower-like structures arranging on the CFP surface (Figure S13d).

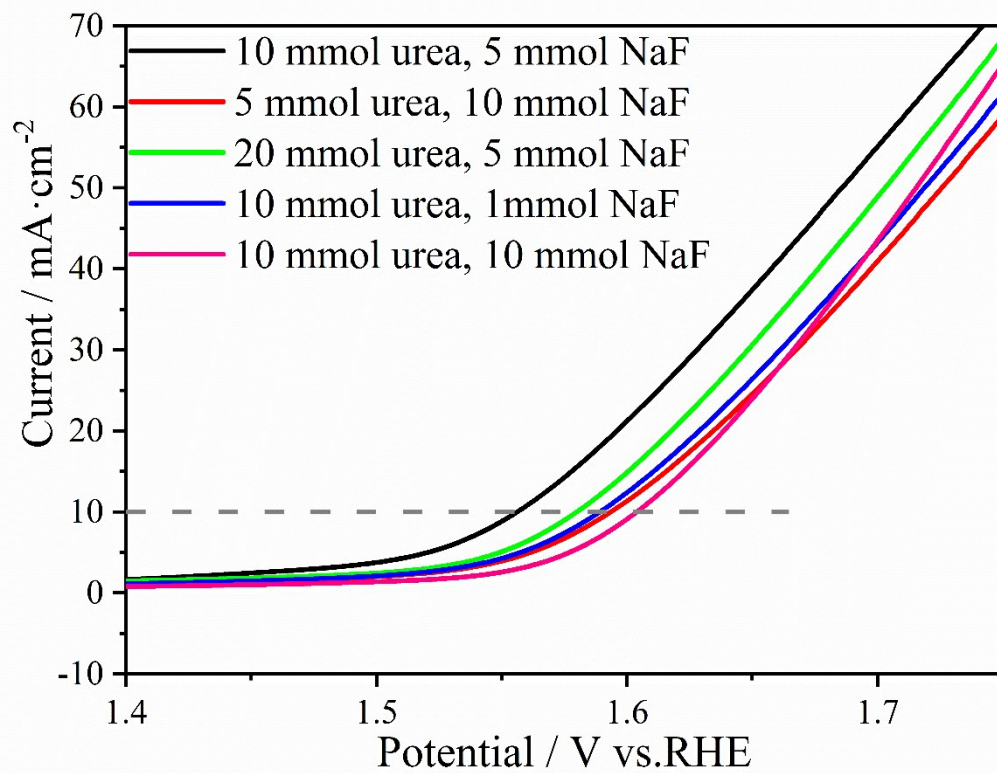


Figure S14. LSV of different urea and NaF ratios.

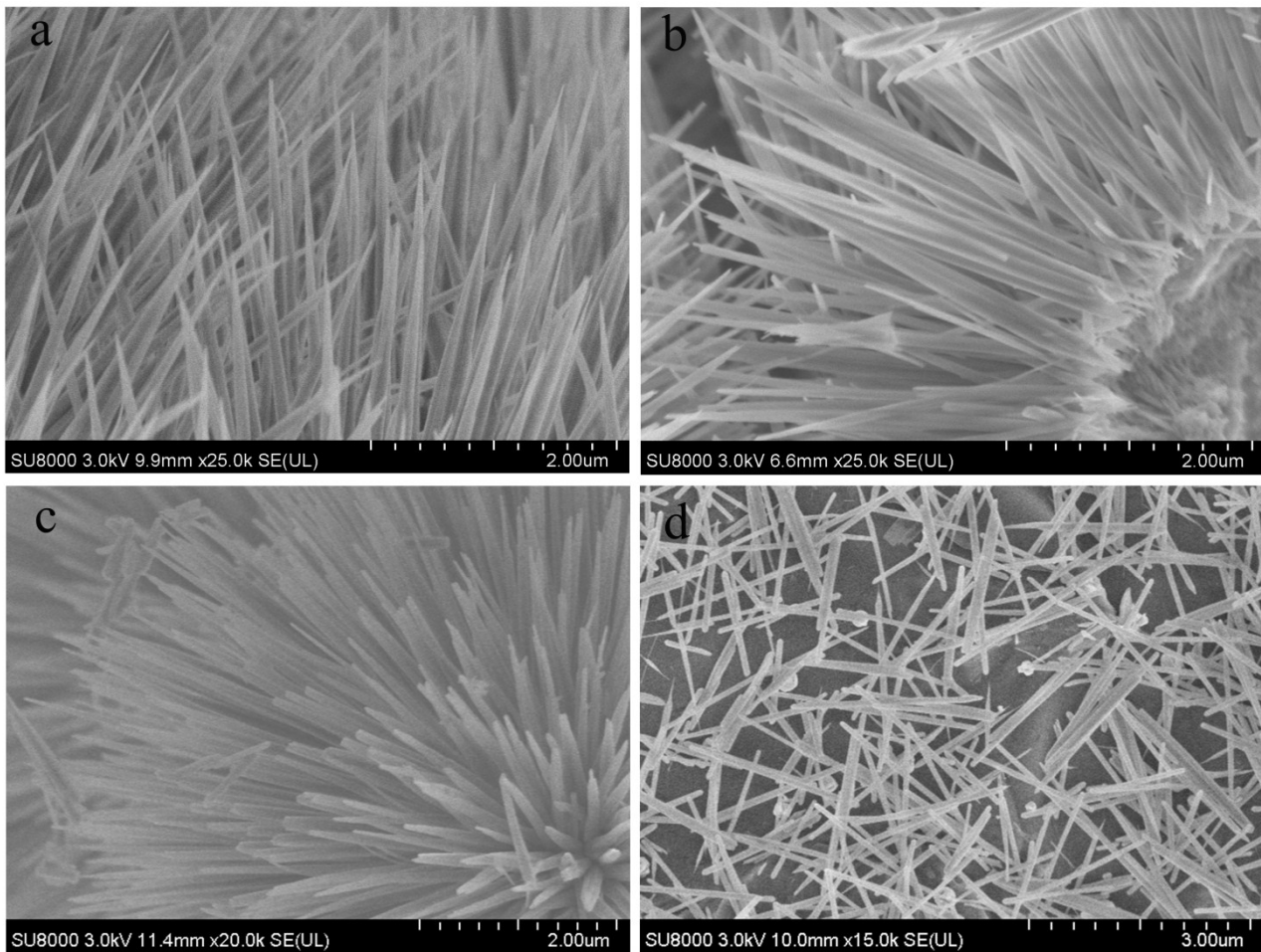


Figure S15. SEM of different time of N:Co(OH)F-CFP

(a) 4h (b) 6h (c) 8h (d) 10h.

In Figure S15, we can see that under the constant condition of 120 °C, different hydrothermal time will have different topography. After 4 h reaction (Figure S15a), the basic structure appeared, but the shape of the spines was too thin then not full enough, it could not be evenly tiled on the CFP. When reaction time was extended to 6 h (Figure S15b), the morphology was found to be a standard cylindrical stab-shaped structure. The original appearance of the structure maintained even after 8h reaction time, but too lush, and the catalytic activity is less robust (Figure S15c);

After 10h reaction, the structure was destroyed (Figure S15d). Some of the white particles on the surface of CFP are part of themselves melted and formed.

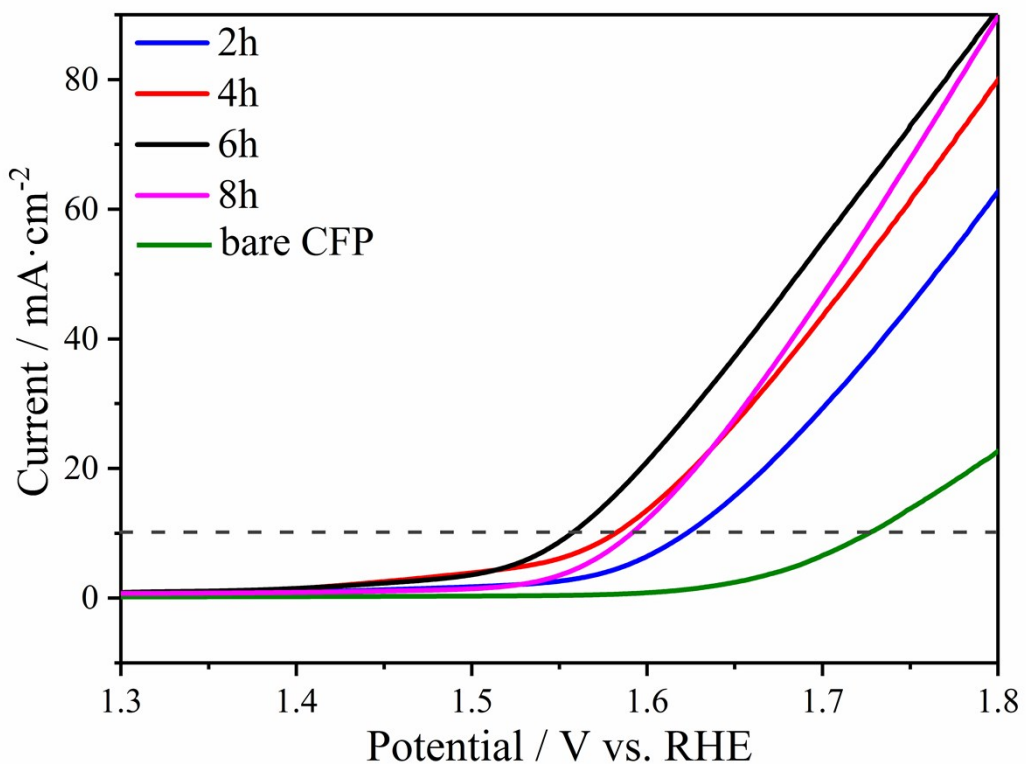


Figure S16. different reaction time of N:Co(OH)F-CFP.

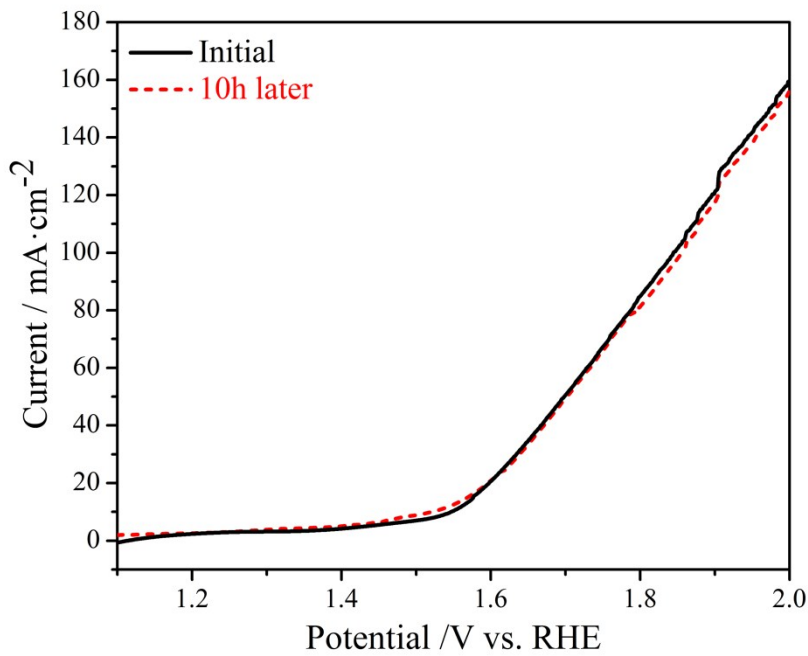


Figure S17. LSV comparison of OER activity before and after IT test.

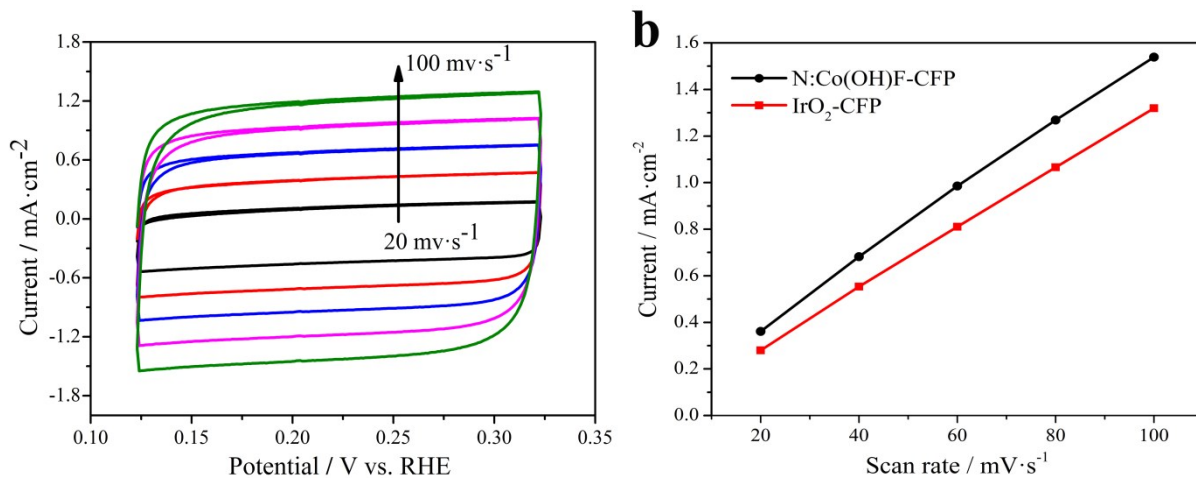


Figure S18. (a) Electrochemical cyclic voltammetry of N:Co(OH)F-CFP at different sweep rates (voltage range: 0.12-0.32 V vs. RHE) (b) Double-layer capacitance curve of N:Co(OH)F-CFP and IrO₂-CFP.

Table S1. XPS full spectrum analysis

1. Co(OH)F-CFP

Name	Peak BE	FWHM	Area (P)	At. %	Q
C1s	284.71	2.5	24902.53	77.59	1
Co2p ₃	780.81	1.3	13638.85	0.37	1
O1s	532.26	0.07	12202.78	21.72	1
F1s	685.43	2.44	438.39	0.33	1

2. N:Co(OH)_x-CFP

Name	Peak BE	FWHN	Area (P)	At. %	Q
C1s	284.73	1.15	24956.41	65.01	1
N1s	400.81	0.14	983.58	1.45	1
Co2p ₃	781.96	2.63	17705.44	3.97	1
O1s	532.4	1.6	32299.42	29.57	1

3. Co(OH)_x-CFP

Name	Peak BE	FWHM	Area (P)	At. %	Q
C1s	284.56	1.15	13718.51	71.53	1
Co2p ₃	780.2	2.69	13638.85	6.12	1
O1s	530.4	1.46	12202.78	22.35	1

Table S2. Comparison of selected Co-containing OER electrocatalysts for different substrates in alkaline media.

Catalyst	Tafel slop (mV dec ⁻¹)	η (mV @10 mAcm ⁻²)	Electrolyte	Substrate	Reference
N:Co(OH)F -CFP	69.75	310	1.0 M KOH	Carbon fiber paper	This work
3D Co(OH)F	52.8	313	1.0 M KOH	GCE	1
CoP@RGO	75	280	1.0 M KOH	GCE	2
CoCr ₂ O ₄ /CNS	51	326	1.0 M KOH	GCE	3
NiCoP/C	96	330	1.0 M KOH	GCE	4
N-doped graphene-CoO	71	340	1.0 M KOH	GCE	5
CoNi(OH) _x nanotubes	77	280	1.0 M KOH	Cu foil	6
Co ₃ O ₄ -carbon nanocomposites	47	346	1.0 M KOH	GCE	7
Co ₃ ZnC/Co@CN	81	366	1.0 M KOH	GCE	8
NiCo LDH	40	367	1.0 M KOH	GCE	9
CoP hollow polyhedron	57	400	1.0 M KOH	GCE	10
Co-P film	47	345	1.0 M KOH	Copper foil	11
Co ₃ O ₄ /NiCo ₂ O ₄ nanocages	88	340	1.0 M KOH	Ni foam	12
CoMn-LDH nanosheets	43	324	1.0 M KOH	GCE	13
Co _{2.25} Cr _{0.75} O ₄	60 ± 3	350	1.0 M NaOH	GCE	14
Co-C ₃ N ₄ /CNT	68.4	380	1.0 M KOH	GCE	15
CoO _x film	42±1	403	1.0 M KOH	Au/Ti or ITO coated glass	16
Co@Co ₃ O ₄ @NMC C/rGO	71	340	1.0 M KOH	GCE	17
CoP ₃ CPs	76	340	1.0 M KOH	Carbon Paper	18
Co(OH) ₂	95	421	1.0 M KOH	Carbon Cloth	19
Co ₂ (OH) ₂ BDC nanosheets	74	273	1.0 M KOH	GCE	20
CoO-MoO ₂ nanocages	69	312	1.0 M KOH	GCE	21

Reference

- 1 S. Wan, J. Qi, W. Zhang, W. Wang, S. Zhang, K. Liu, H. Zheng, J. Sun, S. Wang and R. Cao, *Adv. Mater.*, 2017, **29**, 1700286.
- 2 M. Al-Mamu, X. T. Su, H. M. Zhang, H. J. Yin, P. Liu, H. G. Yang, D. Wang, Z. Y. Tang, Y. Wang and H. J. Zhao, *Small*, 2016, **12**, 2866-2871.
- 3 G. Zhang, G. Wang, Y. Liu, H. Liu, J. Qu and J. Li, *J. Am. Chem. Soc.*, 2016, **138**, 14686-14693.
- 4 P. L. He, X.-Y. Yu and X. W. Lou, *Angew. Chem., Int. Ed.*, 2017, **56**, 3897-3900.
- 5 S. Mao, Z. H. Wen, T. Z. Huang, Y. Hou and J. H. Chen, *Energy Environ. Sci.*, 2014, **7**, 609-616.
- 6 S. Li, Y. Wang, S. Peng, L. Zhang, A. M. Al-Enizi, H. Zhang, X. Sun and G. Zheng, *Adv. Energy Mater.*, 2016, **6**, 1501661-1501667.
- 7 M. Leng, X. Huang, W. Xiao, J. Ding, B. Liu, Y. Du and J. Xue, *Nano Energy*, 2017, **33**, 445-452.
- 8 J. Su, G. Xia, R. Li, Y. Yang, J. Chen, R. Shi, P. Jiang and Q. Chen, *J. Mater. Chem. A*, 2016, **4**, 9204-9212.
- 9 H. Liang, F. Meng, M. Cabán-Acevedo, L. Li, A. Forticaux, L. Xiu, Z. Wang and S. Jin, *Nano Lett.*, 2015, **15**, 1421-1427.
- 10 M. Liu and J. Li, *ACS Appl. Mater. Interfaces*, 2016, **8**, 2158-2165.
- 11 N. Jiang, B. You, M. Sheng and Y. Sun, *Angew. Chem., Int. Ed.*, 2015, **54**, 6251-6254.
- 12 H. Hu, B. Guan, B. Xia and X. W. Lou, *J. Am. Chem. Soc.*, 2015, **137**, 5590-5595.

- 13 F. Song and X. Hu, *J. Am. Chem. Soc.*, 2014, **136**, 16481-16484.
- 14 C.-C. Lin and C. C. L. McCrory, *ACS Catal.*, 2017, **7**, 443-451.
- 15 Y. Zheng, Y. Jiao, Y. H. Zhu, Q. R. Cai, A. Vasileff, L. H. Li, Y. Han, Y. Chen and S. Z. Qiao, *J. Am. Chem. Soc.*, 2017, **139**, 3336-3339.
- 16 L. Trotochaud, J. K. Ranney, K. N. Williams and S. W. Boettcher, *J. Am. Chem. Soc.*, 2012, **134**, 17253-17261.
- 17 X. Li, Y. Fang, L. Wen, F. Li, G. Yin, W. Chen, X. An, J. Jin and J. Ma, *Dalt. Trans.*, 2016, **45**, 5575–5582.
- 18 T. Wu, M. Pi, X. Wang, D. Zhang and S. Chen, *Phys. Chem. Chem. Phys.*, 2017, **19**, 2104–2110.
- 19 X.-F. Lu, P.-Q. Liao, J.-W. Wang, J.-X. Wu, X.-W. Chen, C.-T. He, J.-P. Zhang, G.-R. Li and X.-M. Chen, *J. Am. Chem. Soc.*, 2016, **138**, 8336–8339.
- 20 Y. Xu, B. Li, S. Zheng, P. Wu, J. Zhan, H. Xue, Q. Xu and H. Pang, *J. Mater. Chem. A*, 2018, DOI: 10.1039/c8ta03128b.
- 21 F. Lyu, Y. Bai, Z. Li, W. Xu, Q. Wang, J. Mao, L. Wang, X. Zhang and Y. Yin, *Adv. Funct. Mater.*, 2017, **27**, 1702324.